American Mineralogist, Volume 96, pages 1148–1157, 2011

Orientation of channel carbonate ions in apatite: Effect of pressure and composition

Michael E. Fleet,[1,*] Xiaoyang Liu,[2] and Xi Liu[3]

[1]Department of Earth Sciences, University of Western Ontario, London, Ontario N6A 5B7, Canada
[2]College of Chemistry, Jilin University, Changchun 130012, P. R. China
[3]School of Earth and Space Science, Peking University, Beijing 100871, P. R. China

Abstract

X-ray structure and FTIR spectroscopy evidence is reviewed for two separate orientations of carbonate ions in the **c**-axis channel of carbonate apatite (CHAP) synthesized at high pressure and temperature: A1 carbonate has two O atoms close to the **c**-axis, whereas A2 carbonate has only one. The A2 orientation is reevaluated and its local structure refined using a rigid body model. A2 is the high-pressure configuration, but the A1 → A2 transformation is also dependent on bulk composition, especially the presence of type B carbonate. In the dry CaO-P_2O_5-CO_2 system, the A1 → A2 transformation is initiated beyond about 4 GPa in type A CHAP compared with 1–2 GPa in A-B CHAP. Also, A2 carbonate is only weakly present in Na-bearing A-B CHAP synthesized at 0.5–1 GPa, which is assumed to be close to the threshold pressure for the transformation. The pressure stability of A2 is believed to be related to its central location in the channel and equitable distribution of bond distances to Ca2 cations in the channel wall (2.25 to 2.54 Å).

Keywords: Apatite structure, high-pressure phase transformation, biomineralization, CO_2 sequestration

Introduction

The calcium phosphate apatites [$Ca1_4Ca2_6(PO_4)_6X_2$; with X = F,OH,Cl,O, etc.] (e.g., Pan and Fleet 2002) have importance in both geochemistry and biology. Apatites sequester phosphorus, rare earth elements, actinides, and volatile elements in the Earth's crust and mantle (e.g., O'Reilly and Griffin 2000; Pan and Fleet 2002; Harlov et al. 2002). Also, fluorapatite is a practical host for the containment of high-level nuclear waste, as evidenced by its occurrence in the natural reactor at Oklo, Gabon (e.g., Bros et al. 1996). Within the biosphere, carbonate-bearing hydroxylapatite (presently referred to as carbonate apatite and abbreviated as CHAP) is by far the most important biomineral, accounting for up to about 65 wt% of cortical bone and 97 wt% of dental enamel (Elliott 2002; Wopenka and Pasteris 2005). Fluoride-bearing CHAP is the important anticaries component of dental enamel (Brudevold et al. 1956), and CHAP and carbonated fluorapatite (CFAP; also francolite) are the dominant minerals in phosphorites (McClellan and Lehr 1969).

Calcium apatite minerals are dominantly solid solutions of hydroxylapatite [HAP; ideally $Ca_{10}(PO_4)_6(OH)_2$; $Z = 1$], fluorapatite [FAP; $Ca_{10}(PO_4)_6F_2$], and chlorapatite [CLAP; $Ca_{10}(PO_4)_6Cl_2$]. The natural phases all have the hexagonal space group $P6_3/m$, although pure, end-member HAP and CLAP crystallize in the monoclinic space group $P2_1/b$ (Hughes and Rakovan 2002; White et al. 2005). The $P6_3/m$ structure of calcium apatites is well known. Apatite is an orthophosphate: isolated PO_4 tetrahedra centered at z = (1/4, 3/4) are linked by Ca1 in ninefold (6+3) coordination and Ca2 in an irregular sevenfold (6+1) coordination. A prominent feature of the structure is the large **c**-axis channel that accommodates the X anion component (F,OH,Cl) and is defined by triclusters of Ca2 cations at z = (1/4, 3/4) (Fig. 1). In FAP, the F anion is located on the **c**-axis at z = (1/4, 3/4) in the center of a tricluster of Ca cations. Hydroxyl in HAP and Cl in CLAP are displaced along the **c**-axis and have split atom positions with occupancy of 0.5: the hydroxyl oxygen is at $z = \pm(0.198, 0.302)$ and the much larger Cl anion is displaced further at $z = \pm(0.432, 0.068)$ (Hughes et al. 1989). Thus, the coordination of the X anion is equilateral triangular in FAP but near octahedral in CLAP.

The structural role of carbonate in hydroxylapatite and fluorapatite has been investigated extensively by X-ray powder, X-ray single-crystal, and neutron powder diffraction methods (e.g., Elliott 1994; Suetsugu et al. 2000; Ivanova et al. 2001; Wilson et al. 1999, 2004, 2006; Leventouri et al. 2000, 2001; Antonakos et al. 2007), as well as by infrared, Raman, and nuclear magnetic resonance spectroscopy (e.g., Elliott 1964; Bonel 1972; LeGeros et al. 1969; Rey et al. 1989, 1991; Kim et al. 1996; Cho et al. 2003; Mason et al. 2007, 2009; Fleet et al. 2004; Fleet 2009) and theoretical simulations (Peeters et al. 1997; Peroos et al. 2006). It has been established that the carbonate ion can be accommodated either in the **c**-axis structural channel or as a substituent for the phosphate group: the former carbonate is known as type A and the latter as type B. However, more detailed structure analysis of carbonate apatite using powder diffraction methods has been frustrated by several factors, including: (1) the limited substitution of carbonate (especially of type B carbonate); (2) small (nanoscale) crystal size of biological apatite and apatite precipitated from aqueous solution and of francolite from phosphorites; (3) poor crystallinity; and (4) weak and overlapped electron density of carbonate atoms.

Recently, accommodation of the carbonate ion in Na-free CHAP (Fleet and Liu 2003, 2004, 2005; Fleet et al. 2004),

* E-mail: mfleet@uwo.ca

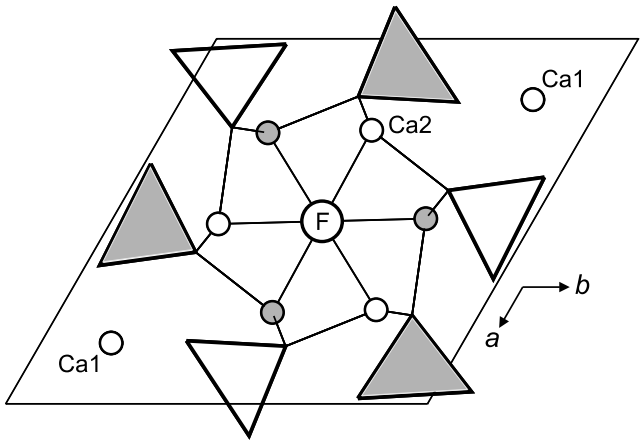

FIGURE 1. Structure of fluorapatite showing triclusters of Ca2 cations in channel wall: circles and triangles are Ca2 and PO_4 groups, respectively, centered at z = 1/4 (shaded) and z = 3/4 (open); unit-cell outline is displaced by (–0.5, –0.5, 0.0).

Na-bearing CHAP (Fleet and Liu 2007), Na-bearing CFAP (Fleet and Liu 2008a), and Na-bearing carbonate chlorapatite (CCLAP; Fleet and Liu 2008b) has been investigated using the X-ray single-crystal structure method in conjunction with Fourier transform infrared spectroscopy (FTIR). This project encompassed a total of 17 single crystals grown from carbonate-rich melts at high temperature and pressure. Crystal compositions corresponded approximately to the substitution formula $Ca_{10-(y+z)}Na_y\square_z[(PO_4)_{6-(y+2z)}(CO_3)_{y+2z}][X_{2-2x}(CO_3)_x]$, where $\square$ is a large cation vacancy and $x \approx y$ up to 1.0 and $z \approx 0.0$ for CHAP, $x \approx y \approx 4z \approx 0.4$ for CCLAP, and $x \approx y \approx 2z \approx 0.1$ for CFAP, for equivalent conditions of synthesis. The sodium cation and A and B carbonate ion defects were locally coupled in all three composition series investigated, to facilitate charge compensation and minimize the effects of spatial accommodation (Fleet and Liu 2007). Crystals of Na-free type A CHAP (x up to 1.0; $y \approx z \approx 0.0$) were trigonal (space group $P\bar{3}$), but all other apatite crystal products were hexagonal ($P6_3/m$). The type A carbonate ion was oriented in the apatite channel with two O atoms close to the **c**-axis (Fleet and Liu 2003, 2005), hereafter labeled A1 orientation, and the type B carbonate ion was located close to the sloping faces of the substituted phosphate tetrahedron, with structural details varying with composition series. A second channel carbonate species (labeled A2) was identified for the first time in high-pressure Na-free type A-B CHAP (Fleet and Liu 2004; Fleet et al. 2004). Deconvolution of the complex band for the out-of-plane bend (ν_2) vibration in FTIR spectra resulted in estimated proportions for total A (A1+A2) and B carbonate ions in good agreement with the corresponding X-ray structure site occupancies (Fleet 2009).

It was also observed that Na has a profound effect on FTIR spectra, shifting the asymmetric stretch (ν_3) doublet band for A1 carbonate to lower wavenumber where it more complexly overlaps the doublet band for B carbonate (Fleet and Liu 2007; Fleet 2009). Reinterpretation of the vibrational spectra of Na-bearing CHAP led to the important conclusion that the proportion of channel carbonate in bioapatites is significantly higher than previously estimated. In fact, it is probable that the labile fraction of carbonate in bioapatites that has an important role in mediating acid-base reactions in the body (cf. Bushinsky et al. 2002), resides in the apatite channel (Fleet 2009; Low et al. 2010). Thus, a detailed understanding of the accommodation of the carbonate ion in the apatite channel is of prime importance to bioapatite research and, more generally, to the sequestration of atmospheric carbon dioxide by rock-forming minerals. The present study evaluates possible locations for the carbonate ion in the apatite channel, reviews the X-ray structure results for the A1 carbonate ion orientation, reevaluates the orientation of the A2 carbonate ion and completes the X-ray structure refinement of synthetic high-pressure A-B CHAP started in Fleet and Liu (2004), discusses evidence for structural change induced at very high pressure, and discusses evidence for an alternative orientation for the A1 carbonate ion in low-pressure CHAP (Suetsugu et al. 2000; Tonegawa et al. 2010).

EXPERIMENTAL PROCEDURES AND CRYSTAL PRODUCTS

Carbonate apatite crystals were grown from a carbonate-rich flux at high pressure and temperature in 3/4 inch assemblies. Experimental conditions are summarized in Tables 1 and 2. Single crystals of Na-free CHAP were prepared by direct reaction of stoichiometric amounts of $Ca_2P_2O_7$ (Alfa Aesar; 98%), CaO (Alfa Aesar; 99.95%), and $CaCO_3$ (Alfa Aesar; 99.99%) in an end-loaded piston-cylinder apparatus (Fleet and Liu 2003, 2004; Fleet et al. 2004). Starting materials

TABLE 1. High-pressure synthesis experiments

Experiment	Starting composition*	*P*† (GPa)	*T*† (°C)	Products		
	Na-bearing A-B CHAP					
LM005	see below	0.5	1200	A1	B	
LM006	see below	1.0	1200	A1	B	
	Na-free A CHAP					
PC71	9:1	2	1400	A1		
PC74	9:1	2	1500	A1		
PC56	9:1	3	1400	A1		
PC16	9:1	4	1400	A1		
	Na-free A-B CHAP					
PC26	6:4	2	1350	A1	B	A2
PC73	8:2	2	1450	A1	B	A2
PC17	8.2	3	1400		B	
PC55	8:2	3	1400	A1	B	A2
PC18	7:3	3	1400	A1	B	A2
PC53	7:3	3	1400‡	A1	B	A2
PC57	7:3	3	1400	A1	B	A2

* Starting composition for Na-free CHAP is proportion of 1/3($Ca_2P_2O_7$+CaO):$CaCO_3$; LM005 is $Ca_8Na_2[(PO_4)_4(CO_3)_2](OH)_2$+fluid; LM006 is $Ca_7Na_3(PO_4)_3(CO_3)_3(OH)_2$+fluid.
† Uncertainties in *P* and *T* are ±0.1 GPa and ±5 °C, respectively.
‡ Followed by annealing at 3 GPa, 1000 °C.

TABLE 2. Amounts of Na and A and B carbonate in selected products* (pfu†)

Apatite	Expt.	*T* (°C)	*P* (GPa)	EPMA Na	X-ray structure A	X-ray structure B	X-ray structure B/A	FTIR‡ B/A
			Na-free synthetic apatites					
CHAP	PC71	1400	2.0	–	0.75(3)	0.11(2)	0.2	0.2
	PC17	1400	3.0	–	0.00(2)	0.17(2)	–	1.3
	PC18	1400	3.0	–	1.08(8)§	0.49(2)	0.5	0.5
	PC55	1400	3.0	–	1.09(4)	0.56(2)	0.5	0.4
			Na-bearing synthetic apatites					
CHAP	LM005	1200	0.5	0.87(3)	1.00(5)	0.77(3)	0.8	0.9
	LM006	1200	1.0	0.35(4)	0.52(3)	0.38(2)	0.7	0.8

* See Fleet and Liu (2003, 2004, 2007, 2008a, 2008b) and Fleet et al. (2004) for details on all high-pressure synthesis experiments and products.
† pfu is per formula unit.
‡ Using ν_2 band.
§ Type A carbonate for PC18 and PC55 is A1+A2.

were mixed in the proportions indicated in Table 1. Calcium pyrophosphate and CaO were dried at 1000 °C for 12 h, and $CaCO_3$ was dried at 200 °C for 12 h. In addition, furnace parts were previously fired at 1000 °C in air. The starting mixture was encapsulated in a sealed platinum tube with a diameter of 5 mm and a height of 12 mm, which was separated by crushable MgO tubing from a graphite tube. Temperature was measured by inserting a Pt-Pt90%Rh10% thermocouple into the high-pressure cell; it was allowed to fluctuate by about ±5 °C to aid crystal growth. The experiments were initially over-pressurized by about 10%, then brought to the correct pressure when the run temperature was attained, and quenched at near-isobaric pressure by switching off the furnace and pumping simultaneously. Single crystals of Na-bearing CHAP, CFAP, and CCLAP were prepared using a Quickpress (Depths of the Earth Co., LLC). Starting compositions for Na-bearing CHAP were prepared from analytical grade $CaHPO_4$, Na_2CO_3, $Ca(OH)_2$, and $CaCO_3$ (Fleet and Liu 2007). These salts were mixed in stoichiometric proportions corresponding to an ideal carbonate apatite formula of $Ca_{10-y}Na_y[(PO_4)_{6-y}(CO_3)_y](OH)_2$ with $y = 2$ or 3 and excess fluid (Table 1). $CaHPO_4$ was used without any drying, but Na_2CO_3, $Ca(OH)_2$, and $CaCO_3$ were dried at 200 °C and 1 atm for 48 h, and the starting mixtures were mixed and ground under acetone in an agate mortar. CaF_2±CaO and $CaCl_2$ were added in place of $Ca(OH)_2$ in the preparation of Na-CFAP (Fleet and Liu 2008a) and Na-CCLAP (2008b), respectively.

Infrared spectra for both hand-separated apatite crystals and bulk products were obtained with a Nicolet Nexus 670 FTIR spectrometer using KBr pellets and hand-separated crystals. Single-crystal X-ray diffraction measurements were made at room temperature and pressure with a Bruker-Nonius Kappa CCD diffractometer and graphite-monochromatized Mo$K\alpha$ X-radiation (50 kV, 32 mA, $\lambda = 0.7107$ Å). The COLLECT software (Nonius 1997) was used for unit-cell refinement and data collection. The reflection data were processed with SORTAV-COLLECT, using an empirical procedure for absorption correction, and SHELXTL/PC (Siemens 1993). Structure refinements were made with LINEX77 (Coppens 1977). Scattering factors for neutral atomic species and values of the anomalous scattering factors f' and f'' were taken, respectively, from Tables 2.2A and 2.3.1 of the *International Tables for X-ray Crystallography* (Ibers and Hamilton 1974). Further experimental details and procedures for data reduction and structure analysis are reported in Fleet and Liu (2003, 2004, 2007, 2008a, 2008b) and Fleet et al. (2004).

Results and discussion

Crystal products

As detailed elsewhere (Fleet and Liu 2003, 2004, 2007, 2008a, 2008b; Fleet et al. 2004), all crystal products had positionally-disordered distributions of carbonate ions in the **c**-axis channel. Unlike atom-for-atom solid solution, substitution of the carbonate ion into apatite introduces new atomic positions and, with the single exception of the carbonate ion perpendicular to the channel length, lowers the local symmetry of the channel anion to $P1$. Thus, there are six equivalent orientations for host structures with $P\bar{3}$ symmetry and 12 for $P6_3/m$ symmetry: since only one orientation can be occupied in any given unit cell, maximum average site occupancies are 0.1667 and 0.0833, respectively. The carbonate ion substituents are replicated by the high symmetry of the host apatite structure and therefore contribute coherent Bragg scattering intensity to the single-crystal diffraction pattern. The diffraction pattern represents only the average structure, a composite of the host structure and the carbonate ions locally ordered in minimum energy locations and configurations. In addition, atoms of the host structure are locally displaced to accommodate the carbonate ions, and this displacement results in anomalous increase in anisotropic displacement parameters, especially for type A-B CHAP (Leventouri et al. 2001; Fleet et al. 2004). As a result of these problems, the X-ray structures of carbonate apatites present numerous challenges in interpretation, especially where carbonate contents are very low. In particular, electron densities appreciably less than that of a hydrogen atom and overlap of carbonate and host structure atoms limit the amount of structural information that can be extracted from X-ray structure analysis. It is emphasized that all crystals investigated were of high-diffraction quality, and the diffraction patterns revealed no evidence of ordering of the carbonate ion defects in the form of superstructure reflections, diffuse scattering or anomalous reflection broadening.

Model structures

The carbonate ion is located in the **c**-axis channel of apatite by bonds between the carbonate O atoms and Ca2 cations in the channel wall. Three possible orientations of the planar carbonate ion are illustrated in Figure 2. These model structures are based on the unit-cell parameters of hydroxylapatite (HAP; Hughes et al. 1989), ideal equilateral triangular geometry of the carbonate ion (O-O = 2.219 Å, C-O = 1.281 Å; Smyth and Bish 1988), and Ca2 cations positioned at (0, 1/4, 1/4) and symmetry equivalent positions for space groups $P6_3/m$ and $P\bar{3}$. Model (a) relates to the orientation of the A1 carbonate ion in type A CHAP (Fleet and Liu 2003, 2005), A-B CHAP (Fleet and Liu 2004, 2007; Fleet et al. 2004), A-B CFAP (Fleet and Liu 2008a), and A-B CCLAP (Fleet and Liu 2008b). The plane of the carbonate ion is normal to the (001) plane and two of the carbonate O atoms (O6 and O7 in Fig. 2a) are located on the **c**-axis. The third (off-axis) O atom and the carbon atom are positioned mid-way along the **c**-axis at $z = 0.5$. Model (b) relates to the orientation of the A2 carbonate ion in high-pressure Na-free A-B CHAP that was first reported in Fleet and Liu (2004) and Fleet et al. (2004) and is presently revised in this study. Again, the plane of the carbonate ion is normal to (001), but now only one carbonate O atom (O10 in Fig. 2b) is located on the **c**-axis, along with the carbon atom at height $z = 0.5$. The other two (off-axis) O atoms are both at $z = 0.593$. In model (c), the carbonate ion is parallel to the **a**-**b** plane, at a height $z = 0.436$, and the carbon atom is located on the **c**-axis. This orientation is thought to be feasible but has not been encountered to date in carbonate apatites.

The model structures for A1 and A2 carbonate ions result in Ca2-O bond distances that are either unrealistic or unequally distributed (Figs. 2a and 2b). However, this situation is improved considerably by minor adjustments in the orientation of the carbonate ions through rotation about the **c**-axis, tilting (canting), and displacement (Figs. 3a and 3b).

A1 carbonate ion

In type A CHAP from experiment PC71 (Table 1), the A1 carbonate ion is rotated 13.6° counterclockwise, as viewed in Figure 2a, and canted 8.8° away from the **c**-axis (see Fig. 2b of Fleet and Liu 2005). The presently calculated Miller indices for the plane of the carbonate ion are $h = -10.5$, $k = 15.4$, $l = 1.77$; i.e., close to $(\bar{2}30)$. In addition, the carbonate ion is displaced away from the channel wall, positioning the carbon atom near the **c**-axis, to extend the Ca2-O distances to 2.17 and 2.38 Å. Although the Ca2-O bond distances have been optimized by the rigid body rotations and displacements of the carbonate ion (Fleet and Liu 2005), the equilateral triangular geometry of the carbonate ion remains incompatible with six Ca2-O distances of equal length. As discussed earlier (Fleet and Liu 2005), the apatite channel cannot accommodate neighboring carbonate ions centered at $z \approx 0.0$ and 0.5. The carbonate ions have to be ordered along the channel at $z \approx 0.5$, leaving the channel location at $z \approx 0.0$ vacant

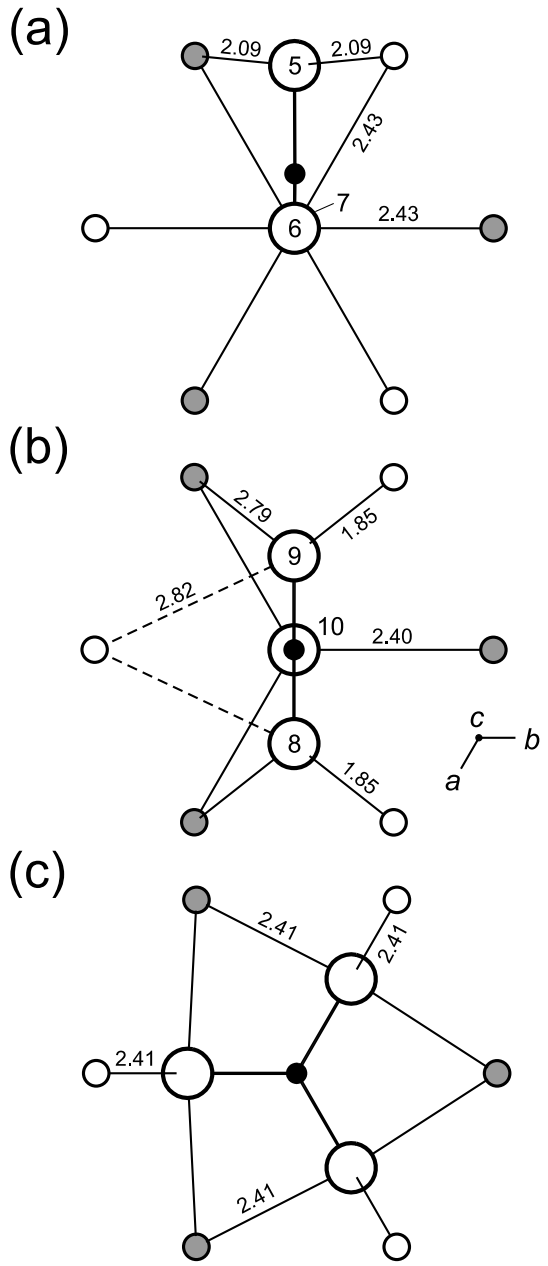

FIGURE 2. Model structures for channel of apatite occupied by carbonate ion oriented (**a**) with two O atoms on the **c**-axis (A1 orientation), (**b**) with one oxygen on the **c**-axis (A2 orientation), and (**c**) perpendicular to **c**-axis: channel is defined by triclusters of Ca2 at z = 1/4 (shaded) and z = 3/4 (open); bond distances are in angstroms.

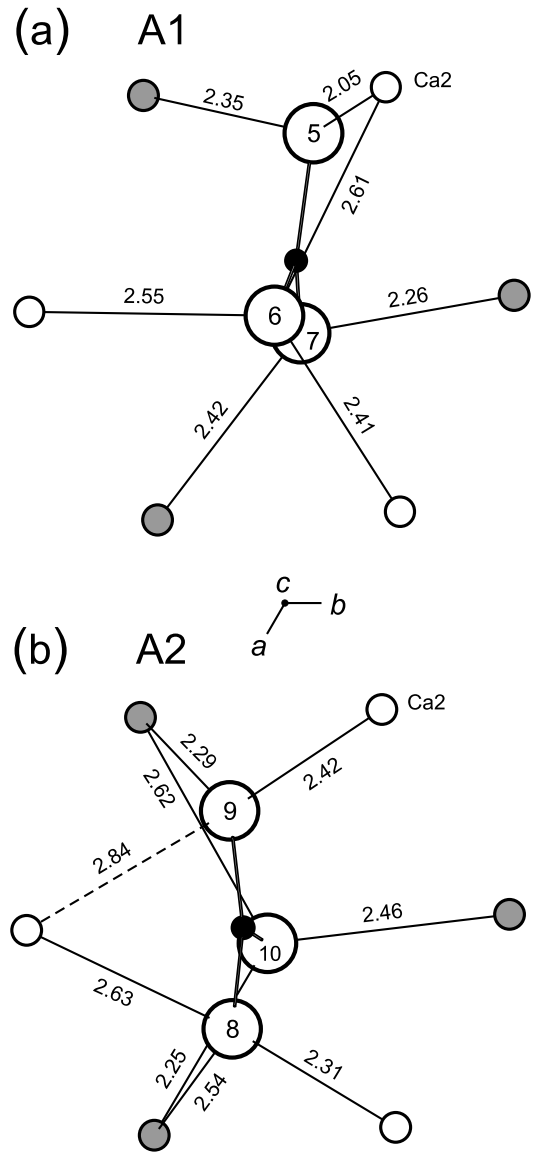

FIGURE 3. Orientation of carbonate ions in Na-free A-B CHAP (PC55): (**a**) A1 carbonate ion; (**b**) A2 carbonate ion; bond distances are in angstroms and estimated standard deviations are <0.01.

and lowering the symmetry of the apatite to $P\bar{3}$. In the type A CHAP of PC71, only three-quarters of the channel locations at z ≈ 0.5 are occupied by carbonate ions, and the electron density is distributed over six equivalent positions in the domain-disordered crystals, resulting in site occupancies of only 0.125 for the four carbonate ion atoms. The remaining charge balance is provided by hydroxyl ions. The overall structural adjustments required to accommodate the bulky carbonate ion in the hydroxylapatite channel are complex and include dilation of the channel at $z \approx 0.5$, constriction of the channel at $z \approx 0.0$, contraction of the $Ca1O_n$ polyhedron, and rigid body rotation of the PO_4 tetrahedron about the P-O1 bond axis (Fleet et al. 2004).

The plane of the A1 carbonate ion of Na-free A-B CHAP from experiment PC55 (Table 1) is canted 7.3° relative to the **c**-axis, similarly to the channel carbonate of type A CHAP, but the plane is now rotated clockwise by 7.4° relative to the model structure of Figure 2a (Fig. 3a). The Miller indices for the plane of the carbonate ion are h = –5.9, k = 15.2, l = 1.42; i.e., close to $(\bar{1}30)$. The difference in orientation compared to that of the A1 carbonate in type A CHAP is probably related to disruption of the basic apatite structure by the introduction of B carbonate ions. Also, in PC55 the apatite channel has to accommodate a marginally excess amount of carbonate (A2 was interpreted to be in a stuffed channel location in Fleet and Liu 2004). The presently refined site occupancies for PC55 are 0.042 for A1 and 0.049

for A2, compared to a total of 0.083 for one carbonate ion per formula unit (pfu). The **c**-axis channel of PC55 was interpreted in Fleet and Liu (2004) to contain a mixed up (but, perhaps, locally ordered) sequence of A1 and A2 carbonate ions and minor OH (or O), with the X-ray diffraction crystal structure representing an average of coherent **c**-axis domains of locally ordered structure.

The **c**-axis channel of Na-bearing A-B CHAP from experiment LM005 (Table 1) was fully occupied by the A1 carbonate ion: the atom site occupancies being very close to the ideal value of 0.083, and A2 carbonate was not detected (Fleet and Liu 2007). The orientation of the A1 carbonate ion was generally similar to that in the Na-free A-B CHAP from PC55: the plane of the carbonate ion is rotated clockwise 13.4° but remains parallel to the **c**-axis [tilt angle =0.0°; see Fig. 4b of Fleet and Liu (2007)], and the Miller indices are h = –31.2, k = 83.7, l = 1.06. This result is a clear indication that the clockwise rotation of the A1 carbonate ion is related to the introduction of significant amounts of type B carbonate.

Fleet and Liu (2005) refined the atom parameters of the channel carbonate of type A CHAP (PC71) using a novel rigid-body procedure and ideal carbonate ion geometry because of the high degree of interaction between the parameters for atoms clustered close to the **c**-axis. In residual electron density maps, there were six overlapped maxima for each of C, O6, and O7 (Fig. 3a; space group $P\bar{3}$). On the other hand, the six maxima representing the off-axis oxygen O5 were well resolved. Thus, preliminary refinement of the three O atoms resulted in satisfactory values for x, y, and z coordinates of O5, and z of O6 and O7. The carbon atom was then located on the line joining O5 to the mid-point of O6-O7, and all the positional parameters of O6 and O7 were adjusted to values corresponding to the ideal equilateral triangular geometry, as detailed in Fleet and Liu (2005). Subsequent refinement with the constraints lifted also resulted in an acceptable structure, but the structure resulting from the constrained refinement was preferred, giving markedly improved residual indices R and R_w and goodness-of-fit parameter S compared to the original structure refinement of Fleet and Liu (2003). The same (rigid-body) procedure was used in the refinement of the structure of the Na-bearing A-B CHAP LM005, where the residual electron density for each of the A1 carbonate atoms was distributed over 12 maxima (space group $P6_3/m$). Atom positions for the A1 carbonate ion of LM005 were used in the structure refinements of Na-bearing A-B CFAP and A-B CCLAP (Fleet and Liu 2008a, 2008b), due to the relatively low amounts of channel carbonate in these apatites. Refinement of the A1 carbonate positions of the Na-free A-B CHAP of PC55 was similarly complicated by weak electron density. In this case, the carbonate atom positions were determined off-line for the ideal geometry after preliminary refinement of the structure (Fleet and Liu 2005). Positional parameters and other details for the constrained X-ray structure refinement of the A1 carbonate ion of PC71, PC55, and LM005 are summarized in Table 3.

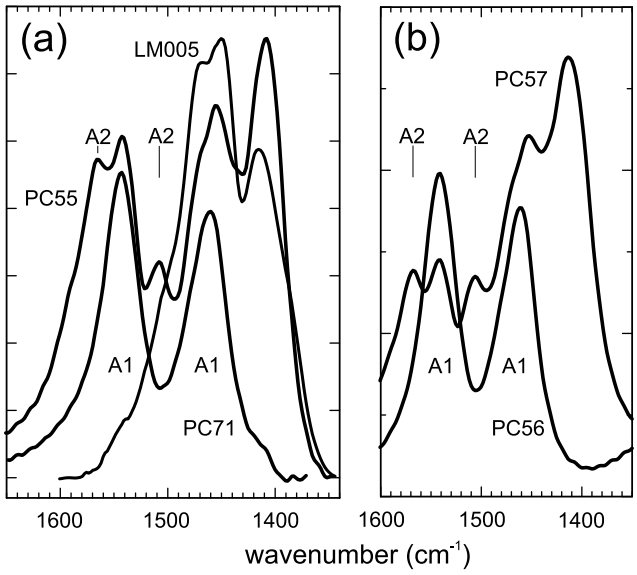

FIGURE 4. FTIR spectra in the asymmetric stretch (ν_3) region for type A CHAP (PC71, PC56), Na-free A-B CHAP (PC55, PC57), and Na-bearing A-B CHAP (LM005): see Table 1 for conditions of synthesis.

Type A2 carbonate ion

The A2 carbonate ion of the Na-free A-B CHAP from experiment PC55 (Fleet and Liu 2004) is rotated 2.1° counterclockwise and canted 10.9° away from the **c**-axis relative to the model structure of Figure 2b, giving Miller indices of h = –14.6, k = 27.4, l = 3.81. Then a slight downward shift to $z \approx 0.45$ for the carbon atom yields a fairly equitable distribution of Ca2-O bond distances (Fig. 3b). Refinement of the atom positions in the original X-ray structure study (Fleet and Liu 2004) was complicated because the A2 orientation resulted in 12 near-equivalent weak residual electron density maxima for O8 and O9, with 12 centered at z = 0.5 and 12 at z = 0.0. Moreover, although O8 and O9 were off-axis O atoms, their electron density maxima in different equivalent orientations of the carbonate ion were in

TABLE 3. Parameters for channel carbonate ions*

Site	Equipoint	Occup.	x	y	z	U,U_{eq}
Na-free A CHAP (PC71): A1 carbonate ion†						
Ca2	6*g*	1.0	0.98964(6)	0.25314(8)	0.24496(7)	0.0224(2)
O5	6*g*	0.125	–0.165(1)	–0.105(1)	0.498(1)	0.059(6)
O6	6*g*	0.125	0.051(1)	0.021(1)	0.688(1)	0.013(3)
O7	6*g*	0.125	0.073(1)	0.072(1)	0.371(1)	0.034(4)
C1	6*g*	0.125	–0.014(1)	–0.004(1)	0.519(1)	0.023(3)
a = 9.5211(3), c = 6.8725(2) Å, $P\bar{3}$; R = 0.025, R_w = 0.021, S = 1.04						
Na-bearing A-B CHAP (LM005): A1 carbonate ion‡						
Ca2	6*h*	0.987(2)	0.9875(1)	0.2499(1)	1/4	0.0181(4)
O5	12*i*	0.0833	–0.220(1)	–0.076(1)	0.472(1)	0.025*
O6	12*i*	0.0833	–0.002(1)	0.003(1)	0.662(1)	0.025*
O7	12*i*	0.0833	0.028(1)	0.018(1)	0.343(1)	0.025*
C1	12*i*	0.0833	–0.065(1)	–0.018(1)	0.492(1)	0.025*
a = 9.3855(7), c = 6.9142(4) Å, $P6_3/m$; R = 0.023, R_w = 0.014, S = 0.60						
Na-free A-B CHAP (PC55): A1 carbonate ion						
Ca2	6*h*	1.0	0.98997(7)	0.25098(7)	1/4	0.0231(3)
O5	12*i*	0.042	–0.205(2)	–0.059(2)	0.479(2)	0.025*
O6	12*i*	0.042(1)	0.015(2)	0.010(2)	0.656(2)	0.025*
O7	12*i*	0.042	0.036(2)	0.048(2)	0.337(2)	0.025*
C1	12*i*	0.042	–0.052(2)	0.000(2)	0.490(2)	0.025*
Na-free A-B CHAP (PC55): A2 carbonate ion						
O8	12*i*	0.049(2)	0.131(2)	0.027(2)	0.565(2)	0.025*
O9	12*i*	0.049	–0.137(2)	–0.109(2)	0.524(2)	0.025*
O10	12*i*	0.065(1)	0.026(2)	0.012(2)	0.272(2)	0.025*
C2	12*i*	0.057(1)	0.007(2)	–0.023(2)	0.454(2)	0.025*
a = 9.5143(3), c = 6.8821(2) Å, $P6_3/m$; R = 0.024, R_w = 0.022, S = 1.33						

* Not refined.
† Fleet and Liu (2003, 2005).
‡ Fleet and Liu (2007).

near coincidence, to the extent that a single atom position was refined in Fleet and Liu (2004). The two separate atom positions were resolved in this study from a combination of refinement, residual electron density, and assumption of ideal carbonate ion geometry. Refinement of the atomic positions (Table 2) for the A2 carbonate ion followed the rigid body procedure used for the A1 carbonate ion. A further complication arose because both O10 and the carbon atom (C2) were very close to the **c**-axis (Fig. 3b), prohibiting independent refinement of their initial parameters. Therefore, a provisional A2 carbonate ion orientation was defined from the refined positions of O8 and O9 and coordinates of O10 calculated assuming ideal geometry. Then O8 was used as the well-refined atom, and C2 was located on the line connecting O8 to the mid-point of O9-O10. The formula amount of A2 carbonate was determined from the site occupancy of O8 (Table 2). The site occupancies of O10 and C2 were refined separately because they were enhanced slightly by interference from minor amounts of other channel constituents situated close to the **c**-axis.

Infrared spectra

The characteristic bands for carbonate occur in the spectral regions 1400–1600 cm^{-1} (asymmetric stretch vibration, ν_3; Fig. 4) and 873–880 cm^{-1} (out-of-plane bend vibration, ν_2; Fig. 5). In addition, a weak band for the stretch vibration of structurally bound OH may be present in CHAP samples near 3572 cm^{-1}. The ν_3 region of the infrared spectra of type A-B CHAP is comprised of complexly overlapped contributions from the A and B carbonate ion species. The ν_3 vibration is twofold degenerate for the free carbonate ion but is represented by a doublet in apatite spectra because the degeneracy is lifted for site symmetries lower than trigonal. For Na-free type A CHAP synthesized at high pressure (e.g., PC71 in Tables 1 and 2), the ν_3 region consisted of a symmetrical doublet with limbs centered at 1544 and 1461 cm^{-1} (Fleet and Liu 2003). The spectra of A-B CHAP from the same series of experiments (e.g., PC55) were complex, but six individual bands were generally recognized by five definite peaks and a prominent shoulder (Fig. 4; Fleet and Liu 2004; Fleet et al. 2004). Initial assignments attributed the strong peak near 1409 cm^{-1} to one limb of the B carbonate ion doublet enhanced by calcite contamination. However, this interpretation was revised by Fleet (2009), who attributed all of the intensity of the 1409 cm^{-1} band to B carbonate, based largely on the absence of the calcite band in the ν_2 spectral region. The 1540 cm^{-1} band is clearly A1, and the stuffed channel carbonate (A2) is characterized by the doublet bands at 1569 and 1507 cm^{-1}. Nevertheless, there is no clear basis for proportioning the absorption in the 1470–1455 cm^{-1} interval between A1 and B carbonate, even with knowledge of the actual (A1, A2, and B) site occupancies obtained from the X-ray structures. In the Na-bearing A-B CHAP, A-B CFAP, and A-B CCLAP crystals synthesized at high pressure (Fleet and Liu 2007, 2008a, 2008b), the ν_3 doublet for the A1 carbonate ion, which is expected from the X-ray structure results to be an important feature, is seemingly shifted to lower wavenumber into the region normally associated with type B carbonate (Fig. 4a). These spectra for the synthetic Na-bearing crystals are similar to those of CHAP precipitated from basic solution, dental enamel, and cortical bone (Elliott 2002; Rey et al. 1989, 1991), and they were previously considered to represent the dominant presence of B carbonate.

In apatite biomaterials, the ν_2 region is normally deconvoluted to give a singlet band for A1 carbonate at 878 cm^{-1} and bands for B carbonate at 871 and 866 cm^{-1} (Rey et al. 1989, 1991). The composite ν_2 band for laboratory synthesized low-pressure CHAP crystals has components for A1 carbonate at 878–881 cm^{-1} and type B at 870–873 cm^{-1} (Elliott 1994; Rey et al. 1989). The ν_2 spectra for high-pressure synthesized CHAP were interpreted in Fleet (2009) by fitting Gaussian components to peaks and prominent shoulders. For Na-free A CHAP (PC71) and Na-bearing A-B CHAP (LM005), the ν_2 spectra were fitted by two bands, one for A1 carbonate at 878 cm^{-1} and one for B carbonate at 870 cm^{-1} (Figs. 5a and 5c). The fitted ν_2 spectrum for PC71 confirms that this well-investigated type A CHAP does contain a small proportion of B carbonate, which is not accounted for in the detailed X-ray structure investigations (Fleet and Liu 2003,

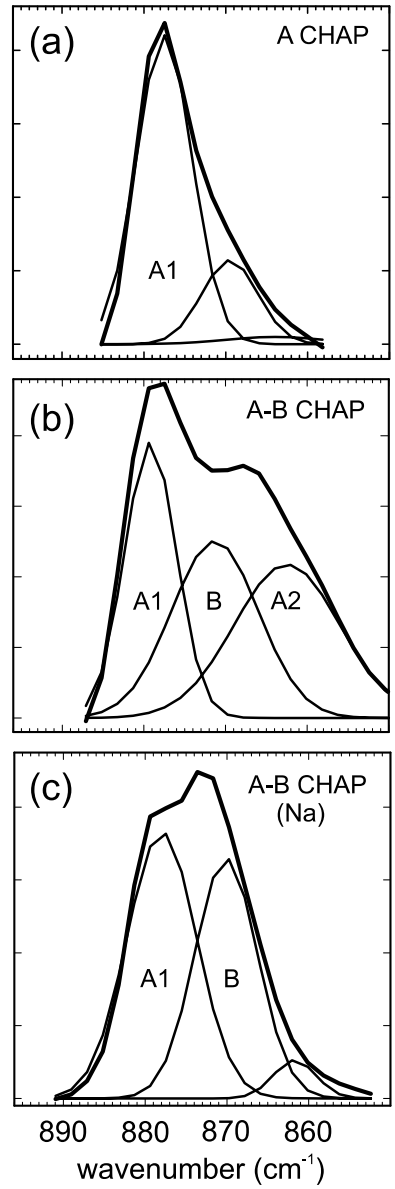

Figure 5. FTIR spectra in the out-of-plane bending (ν_2) region showing fitted Gaussian components: (**a**) PC71; (**b**) PC55; (**c**) LM005.

2005). The ν_2 spectrum for Na-free A-B CHAP (PC55) was fitted to three bands, at about 879, 871, and 862 cm^{-1} and assigned to A1, B, and A2 carbonate, respectively (Fig. 5b). The assignment of the stuffed channel species A2 to the band at about 862 cm^{-1} in Na-free A-B CHAP is based largely on the correlated decrease in intensity of this band with decrease in the A2 doublet bands of corresponding ν_3 spectra when PC55 (Fleet and Liu 2004) and PC17 (Fleet et al. 2004; Fleet 2009; Table 1) were annealed at lower temperatures. The resulting proportions of the A1, A2, and B carbonate ion species for PC55 are 31:35:34 and in very good agreement with the proportions of 30:36:34, respectively, obtained for the present X-ray structure site occupancies. Note that the proportion of A2 carbonate is underestimated by peak intensity in the ν_3 spectral region (Fig. 4) because the band components are broad and diffuse.

Fleet (2009) has previously shown that the area ratios B/(A1+A2) of the fitted ν_2 band components are in very good linear agreement with the corresponding quantities calculated from the X-ray structure site occupancies. The proportions of A and B carbonate ions in these high-pressure carbonate apatites are now firmly established by two independent methods, FTIR ν_2 band areas and X-ray structure analysis (Fleet and Liu 2003, 2004, 2007; Fleet et al. 2004). This agreement also establishes FTIR ν_2 band areas as a viable independent method for estimating the proportion of A and B carbonate in CHAP precipitated from aqueous solutions, apatite biominerals, and francolites, and it reinforces earlier studies on biological CHAP (Rey et al. 1989, 1991; Kim et al. 1996).

An important conclusion for this study is that infrared band positions for the A carbonate ions of Na-free CHAP are very sensitive to orientation in the apatite channel but relatively insensitive to the local Ca^{2+} cation environment in the channel wall. The ν_3 doublet for the A2 carbonate ion, which has one O atom near the **c**-axis (Fig. 3b), is shifted significantly to higher wavenumber (1569 and 1507 cm^{-1}) relative to the A1 carbonate ion that has two O atom near the *c*-axis (Fig. 3a). Also, the A2 band for out-of-plane bending (ν_2) is shifted about 17 cm^{-1} to lower wavenumber.

The infrared spectra were also useful in establishing that CO_3^{2-} and OH^- were the only channel anion (X) species present in significant amounts in the synthetic CHAP crystals. The OH stretch band and OH libration band (near 631 cm^{-1}) show a systematic decrease in intensity with increase in carbonate content, with carbonate content estimated from both ν_3 band area and X-ray site occupancies. This inverse correlation is well illustrated in Figure 2 of Fleet and Liu (2007), which displays infrared spectra for a series of Na-bearing CHAP compositions. The OH libration band is prominent for LM002 with 3.8 wt% CO_2 but absent for LM005 with 11.1 wt% CO_2 and all channel locations for the A1 carbonate ion statistically filled (Table 3). In addition, for Na-free CHAP, Figure 3 of Fleet et al. (2004) shows that the libration band is prominent for PC17 with no detectable A1 carbonate content (Table 2) and reduced to a very weak shoulder for PC18 with (A1+A2) > 1.0. The OH stretch band is either absent or very weak for Na-bearing CFAP [Fig. 1 of Fleet and Liu (2008a)] and the libration band is absent for Na-bearing CCLAP [Fig. 3 of Fleet and Liu (2008b)], showing that the channel anions in both of these composition series were essentially only halide and carbonate.

Effect of composition and high pressure

In Fleet and Liu (2004) and Fleet et al. (2004), it was assumed that the A2 carbonate ion orientation was a high-pressure feature because significant amounts of it were present only at the highest pressures investigated (i.e., >2 GPa; Table 1). However, the correlation with pressure is not exclusive because the type A CHAP samples PC16 and PC56 (Fig. 4b) were synthesized at 4 and 3 GPa, respectively, and PC16 has only a minor content of A2 carbonate and PC56 has none [see Fig. 2 of Fleet et al. (2004)]. Also, bands possibly attributable to the A2 carbonate ion are weakly present in infrared spectra of low-pressure CHAP in other studies, both as a sharp peak or shoulder at about 1500 cm^{-1} and diffuse absorption at higher frequency (Nelson and Featherstone 1982; Vignoles et al. 1988; Barralet et al. 1998; Suetsugu et al. 1998). Similarly, the 866 cm^{-1} component in ν_2 band spectra of various bone samples and laboratory synthesized bioapatites, which was identified with the labile carbonate component (Rey et al. 1989, 1991), may correspond to A2 carbonate as well. Alternatively, these weak features may be attributable to disorder of channel carbonate in poorly crystalline materials. For the present CHAP materials, where the association of the anomalous features in FTIR spectra with a second channel orientation has been confirmed, it remains possible that the A2 orientation is not a high-pressure-temperature equilibrium product but instead represents disruption of the channel structure on quenching from high pressure. However, the observations that significant amounts of A2 carbonate are restricted to A-B CHAP and the A2/A1 band area ratio in ν_3 spectra increases with increase in pressure and B carbonate ion content [Table 1; Fig. 2 of Fleet et al. (2004)] suggest otherwise. Note also that whereas annealing of PC55 product in air at 1000 °C resulted in a systematic decrease in A2 carbonate, annealing of PC53 (Table 1) under pressure at the same temperature had no evident effect. The summary results in Table 1 suggest that the A1 → A2 transformation is initiated at or beyond 4 GPa at low total carbonate content and at 1–2 GPa in the presence of B carbonate (type A-B CHAP). Furthermore, the A2 orientation is only weakly present in Na-bearing type A-B CHAP synthesized at 0.5–1 GPa, which is assumed to be close to the threshold pressure for the transformation.

The compositional control on the uptake of A2 and B carbonate by high-pressure synthesized CHAP is interesting and has not been discussed in previous papers. For the experiments on Na-free CHAP, the starting compositions were mixtures of $1/3(Ca_2P_2O_7+CaO)$ and $CaCO_3$ in proportions of 9:1 to 6:4. In experiments at pressures ranging from 2 to 4 GPa, the 9:1 starting composition, which is equivalent to a formula of $Ca_{10}(PO_4)_6(CO_3)$, yielded type A CHAP, with the carbonate ion exclusively in the A1 orientation, whereas 8:2 to 6:4 starting compositions resulted in type A-B CHAP±calcite±melt, with the channel carbonate in both A1 and A2 orientations, over a similar range in pressure (Table 1). This result indicates that the carbonate ion has a strong preference for the apatite channel and only substitutes extensively for the phosphate group when all available channel sites are filled. In summary, the A2 orientation is associated, directly or indirectly, with the formation of B carbonate at high pressure. In the dry $CaO-P_2O_5-CO_2$ system, pressure-induced transformation to the A2 carbonate orientation appears to require excess amounts of $CaCO_3$ to first generate

B carbonate ions. Of course, when most of the channel anion sites are blocked by other common X anion substituents (e.g., OH, F, Cl), B carbonate alone may be formed at relatively low $CaCO_3$ contents.

Investigation of the Na-bearing apatites synthesized at high pressure (A-B CHAP, A-B CFAP, and A-B CCLAP; Fleet and Liu 2007, 2008a, 2008b) revealed strong evidence favoring the local coupling of Na and A1 and B carbonate ion defects. The A1 and B carbonate ion substituents tend to be coupled because the off-axis O atom of the A1 carbonate (O5; e.g., Fig. 3a) is pushed close to the channel wall and close to an O3 O atom of an adjacent PO_4 group. But this impingement is relaxed when O5 is positioned adjacent to either the O3 oxygen vacancy or the displaced O3 O atom resulting from the carbonate-for-phosphate substitution

$$0.5^{Ca}\square + {}^{B}CO_3 = 0.5Ca + PO_4 \quad (1)$$

[see Fig. 5 of Fleet and Liu (2007)]. Of the six possible orientations available, due to the hexagonal symmetry of the host lattice (Figs. 2 and 3), the A1 carbonate ion favors the orientation that places O5 nearest to the B carbonate ion. As noted in Fleet and Liu (2007), the coupling of the third member of the cluster (Na) with type A and B carbonate is probably indirect since the Na cation introduced in the charge-balancing substitution

$$Na + {}^{B}CO_3 = Ca + PO_4 \quad (2)$$

is best positioned close to the O3 vacancy. An explanation for the pressure dependence of the orientation of channel carbonate ions follows from comparison of the local structure of the A1 and A2 orientations (Fig. 3), which shows that impingement with the channel wall is essentially eliminated for the A2 orientation because it is more centrally located in the apatite channel. Thus, there must be a tendency for A1 carbonate ions to roll over to the A2 orientation at high pressure.

Discussion of the Na-bearing experiments highlights the role of minor amounts of Na in limiting the labile fraction of carbonate in bioapatites. Although the labile fraction of bioapatites and low-pressure CHAP is logically associated with the high wavenumber absorption in ν_3 region FTIR spectra, its association with an orientation different from that of A1 carbonate has yet to be confirmed. Nevertheless, A2 carbonate is expected to contribute to the labile fraction of CHAP, regardless of its origin, because of its weaker binding with the channel wall. Finally, it is noteworthy that synthetic Na-bearing type A-B CHAP with $x \approx y \approx 0.5$ [e.g., experiment LM006, Table 2; Fleet and Liu (2007)] is similar in both chemical composition and FTIR spectrum to biological apatite. This agreement confirms that the quenched Na-bearing high-pressure CHAP products with channel carbonate oriented with two O atoms near the **c**-axis are the appropriate analogues for the overall structural features of bioapatite. It is not too surprising that the basic bioapatite structure is reproduced by high-pressure synthesis, given the extensive pressure-temperature stability field of apatite. In the present study, high temperature was required to yield crystals of a size suitable for X-ray structure analysis and high pressure to confine CO_2-rich fluid and vapor. Of course, moderate confining pressure is adequate for growing A1-rich CHAP from a $CaCO_3$-rich flux (Suetsugu et al. 1998) but this study suggests that high pressure is required to yield A-B CHAP with high contents of both B and A2 carbonate.

Symmetry of type A CHAP

Suetsugu et al. (1998) synthesized 1 mm long prismatic crystals of A-B CHAP using a $CaCO_3$ flux under an argon gas pressure of 55 MPa. Channel carbonate was dominant, although the content of B carbonate was also appreciable. The space group was reported as $P\overline{6}$ for the domain-disordered crystals. X-ray single-crystal structure analysis suggested that the A carbonate ion was oriented with only one O atom close to the **c**-axis (Suetsugu et al. 2000). This orientation was similar to that of A2 carbonate in the high-pressure synthesized Na-free A-B CHAP and clearly different from that of the A1 carbonate ion in type A CHAP and A-B CHAP discussed presently. However, this proposed channel structure is inconsistent with the infrared spectrum for the $P\overline{6}$ CHAP that has ν_3 bands at 1540 and 1454 cm^{-1} and ν_2 bands at 882 and 873 cm^{-1}, indicative of A1 and B carbonate ions. As discussed above, the A2 carbonate ion orientation should result in ν_3 bands near 1569 and 1507 cm^{-1} and ν_2 bands near 862 cm^{-1}. Based solely on the infrared data, the channel carbonate ion in the A-B CHAP of Suetsugu et al. (1998, 2000) should be assigned to an orientation with two O atoms close to the **c**-axis.

Fleet et al. (2004) have previously pointed out that Suetsugu et al. (2000) did not investigate the possibility that their crystal symmetry might be $P\overline{3}$ and noted that their thermal parameters (U_{ii}) ranging up to 0.38 $Å^2$ for the off-axis carbonate O atoms were too large for meaningful refinement of the channel carbonate ion. Suetsugu et al. (1998) did show that the crystal symmetry was not restricted by space group extinctions, but their observations are equally consistent with $P\overline{3}$ symmetry, as well as $P\overline{6}$. Importantly, they did not report a statistical analysis of equivalent reflections (reflection multiplicity) to distinguish between these two possible space groups. For example, using SHELXTL for reduction of the raw reflection data of the type A CHAP of PC71 (Fleet and Liu 2003), the combined figure of merit for reflection equivalents was 2.6 for $P\overline{3}$ and 74.6 for $P\overline{6}$, clearly favoring space group $P\overline{3}$ by a wide margin.

Suetsugu et al. (2000) also showed that their $P\overline{6}$ structure accounted for essentially all of the electron density in their crystal. However, their difference Fourier map for the positionally disordered structure with the channel anions omitted [Fig. 1 of Suetsugu et al. (2000)] shows four strong residual electron density maxima along the 00z row, consistent with a channel carbonate ion having two O atoms near the **c**-axis. This feature is unlikely to be attributable to twinning because, in detail, the two peaks at about (0, 0, ±0.44) have a different shape and are more intense than the two generated by the space group $P\overline{6}$ at (0, 0, ±0.06) (equipoint 2g). Moreover, both pairs of maxima disappeared in Suetsugu et al. (2000) when an O atom was placed at $z \approx \pm 0.06$, a response consistent with error in assigning space group symmetry and could arise, for example, if the crystal symmetry were actually $P\overline{3}$ but the raw reflection list had been averaged for Laue class 6/m. This suggestion has been tested using the reflection data for PC71 and the $P\overline{6}$ structure of Suetsugu et al. (2000),

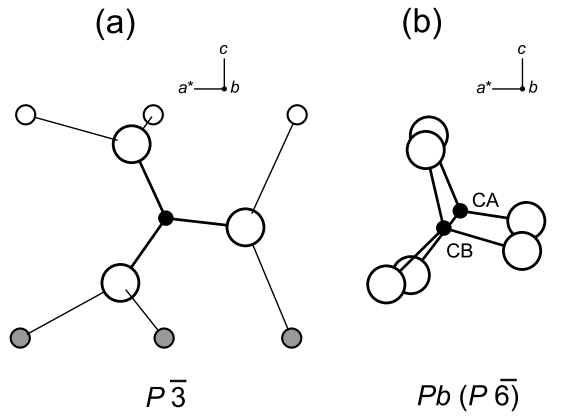

FIGURE 6. Orientation of channel carbonate in: (**a**) $P\overline{3}$ type A CHAP of Fleet and Liu (2003, 2005; PC71), and (**b**) monoclinic *Pb* structure of Tonegawa et al. (2010).

and found indeed to result in the anomalous features presently discussed. When the single axial oxygen is omitted, two pairs of residual electron density maxima are present and are reduced to background values after the electron density map is recalculated with the axial O atom replaced at either $z \approx \pm 0.06$ or $z \approx \pm 0.44$.

Very recently, type A CHAP has been prepared by heating HAP in an atmosphere of CO_2 at 900 °C and the structure reinvestigated by Rietveld powder X-ray diffraction in space group *Pb* (Tonegawa et al. 2010). The FTIR spectrum has ν_3 bands at 1539 and 1467 cm^{-1} and ν_2 at 879 cm^{-1}, in good agreement with PC71 (Fleet and Liu 2003). The *Pb* structure has two independent channel carbonate ions, and both are oriented with two O atoms close to the monoclinic **c**-axis, which is equivalent to the orientation of the A1 carbonate ion in the $P\overline{3}$ structure of PC71 (Fleet and Liu 2003), as illustrated in Figure 6. Note that discrepancies in detailed comparison between PC71 and the *Pb* structure are attributable to the more limited resolution of the Rietveld powder refinement method.

ACKNOWLEDGMENTS

I thank John Hughes, Francis McCubbin, and a third unnamed reviewer for helpful comments, and the Natural Sciences and Engineering Research Council of Canada for financial support.

REFERENCES CITED

Antonakos, A., Liarokapis, E., and Leventouri, T. (2007) Micro-Raman and FTIR studies of synthetic and natural apatites. Biomaterials, 28, 3043–3054.

Barralet, J., Best, S., and Bonfield, W. (1998) Carbonate substitution in precipitated hydroxyapatite: An investigation into the effects of reaction temperature and bicarbonate ion concentration. Journal of Biomedical Materials Research, 41, 79–86.

Bonel, G. (1972) Contribution à l'étude de la carbonatation des apatites. I. Synthèse et étude des propriétés physico-chimiques des apatites carbonatées du type A. Annales de Chimie (Paris, France), 7, 65–88.

Bros, R., Carpena, J., Sere, V., and Beltritti, A. (1996) Occurrence of Pu and fissiogenic REE in hydrothermal apatites from the fossil nuclear reactor 16 at Oklo (Gabon). Radiochimica Acta, 74, 277–282.

Brudevold, F., Gardner, D.E., and Smith, F.A. (1956) Distribution of fluorine in human enamel. Journal of Dental Research, 35, 420–429.

Bushinsky, D.A., Smith, S.B., Gavrilov, K.L., Gavrilov, L.F., Li, J., and Levi-Setti, R. (2002) Acute acidosis-induced alteration in bone bicarbonate and phosphate. American Journal of Physiology-Renal Physiology, 283, F1091–F1097.

Cho, G., Wu, Y., and Ackerman, J.L. (2003) Detection of hydroxyl ions in bone mineral by solid state NMR spectroscopy. Science, 300, 1123–1127.

Coppens, P. (1977) LINEX77. State University of New York, Buffalo, New York, U.S.A.

Elliott, J.C. (1964) The interpretation of the infra-red absorption spectra of some carbonate-containing apatites. In R.W. Fearnhead and M.V. Stack, Eds., Tooth enamel: Its Composition, properties, and fundamental structure, p. 20–22. John Wright and Sons, Bristol, U.K.

——— (1994) Structure and Chemistry of the Apatites and Other Calcium Orthophosphates, 389 p. Elsevier, Amsterdam.

——— (2002) Calcium phosphate biominerals. In M.J. Kohn, J. Rakovan, and J.M. Hughes, Eds., Phosphates, 48, p. 427–453. Reviews in Mineralogy and Geochemistry, Mineralogical Society of America, Chantilly, Virginia.

Fleet, M.E. (2009) Infrared spectra of carbonate apatites: ν_2-region bands. Biomaterials, 30, 1473–1481.

Fleet, M.E. and Liu, X. (2003) Carbonate apatite type A synthesized at high pressure: new space group (*P*3̄) and orientation of channel carbonate ion. Journal of Solid State Chemistry, 174, 412–417.

——— (2004) Location of type B carbonate ion in type A-B carbonate apatite synthesized at high pressure. Journal of Solid State Chemistry, 177, 3174–3182.

——— (2005) Local structure of channel ions in carbonate apatite. Biomaterials, 26, 7548–7554.

——— (2007) Coupled substitution of type A and B carbonate in sodium-bearing apatite. Biomaterials, 28, 916–926.

——— (2008a) Accommodation of the carbonate ion in fluorapatite synthesized at high pressure. American Mineralogist, 93, 1460–1469.

——— (2008b) Type A-B carbonate chlorapatite synthesized at high pressure. Journal of Solid State Chemistry, 181, 2494–2500.

Fleet, M.E., Liu, X., and King, P.L. (2004) Accommodation of the carbonate ion in apatite: An FTIR and X-ray structure study of crystals synthesized at 2–4 GPa. American Mineralogist, 89, 1422–1432.

Harlov, D.E., Foerster, H-J., and Nijland, T.G. (2002) Fluid-induced nucleation of (Y+REE)-phosphate minerals within apatite; nature and experiment. American Mineralogist, 87, 245–261.

Hughes, J.M. and Rakovan, J. (2002) The crystal structure of apatite, $Ca_5(PO_4)_3(F,OH,Cl)$. In M.J. Kohn, J. Rakovan, and J.M. Hughes, Eds., Phosphates, 48, p. 1–12. Reviews in Mineralogy and Geochemistry, Mineralogical Society of America, Chantilly, Virginia.

Hughes, J.M., Cameron, M., and Crowley, K.D. (1989) Structural variations in natural F, OH, and Cl apatites. American Mineralogist, 74, 870–876.

Ibers, J.A. and Hamilton, W.C., Eds. (1974) International Tables for X-ray Crystallography, vol. IV, 366 p. Kynoch Press, Birmingham, U.K.

Ivanova, T.I., Frank-Kamenetskaya, O.V., Kol'tsov, A.B., and Ugolkov, V.L. (2001) Crystal structure of calcium-deficient carbonated hydroxyapatite. Thermal decomposition. Journal of Solid State Chemistry, 160, 340–349.

Kim, H-M., Rey, C., and Glimcher, M.J. (1996) X-ray diffraction, electron microscopy, and Fourier transform infrared spectroscopy of apatite crystals isolated from chicken and bovine calcified cartilage. Calcified Tissue International, 59, 58–63.

LeGeros, R.Z., Trautz, O.R., Klein, E., and LeGeros, J.P. (1969) Two types of carbonate substitution in the apatite structure. Experimentia, 25, 5–7.

Leventouri, T., Chakoumakos, B.C., Moghaddam, H.Y., and Perdikatsis, V. (2000) Powder neutron diffraction studies of a carbonate fluorapatite. Journal of Materials Research, 15, 511–517.

Leventouri, T., Chakoumakos, B.C., Papanearchou, N., and Perdikatsis, V. (2001) Comparison of crystal structure parameters of natural and synthetic apatites from neutron powder diffraction. Journal of Materials Research, 16, 2600–2606.

Low, H.R., Ritter, C., and White, T.J. (2010) Crystal structure refinements of the 2*H* and 2*M* pseudomorphs of ferric carbonate-hydroxyapatite. Dalton Transactions, 39, 6488–6495.

Mason, H.E., Kozlowski, A., and Phillips, B.L. (2007) Solid-state NMR study of the role of H and Na in AB-type carbonate hydroxylapatite. Chemistry of Materials, 20, 294–302.

Mason, H.E., McCubbin, F.M., Smirnov, A., and Phillips, B.L. (2009) Solid-state NMR and IR spectroscopic investigation of the role of structural water and F in carbonate-rich fluorapatite. American Mineralogist, 94, 507–516.

McClellan, G.H. and Lehr, J.R. (1969) Crystal chemical investigation of natural apatites. American Mineralogist, 54, 1374–1391.

Nelson, D.G.A. and Featherstone, J.D.B. (1982) Preparation, analysis, and characterization of carbonated apatites. Calcified Tissue International, 34, S69–S81.

Nonius (1997) COLLECT Software. Nonius, Delft, The Netherlands.

O'Reilly, S.Y. and Griffin, W.L. (2000) Apatite in the mantle: Implications for metasomatic processes and high heat production in Phanerozoic mantle. Lithos, 53, 217–232.

Pan, Y. and Fleet, M.E. (2002) Compositions of the apatite-group minerals: Substitution mechanisms and controlling factors. In M.J. Kohn, J. Rakovan, and J.M. Hughes, Eds., Phosphates, 48, p. 13–49. Reviews in Mineralogy and Geochemistry, Mineralogical Society of America, Chantilly, Virginia.

Peeters, A., De Maeyer, E.A.P., Van Alsenoy, C., and Verbeeck, R.M.H. (1997) Solids modeled by ab initio crystal-field methods. 12. Structure, orientation and position of A-type carbonate in a hydroxyapatite lattice. Journal of Physical

Chemistry B, 101, 3995–3998.
Peroos, S., Du, Z., and de Leeuw, N.H. (2006) A computer modelling study of the uptake, structure and distribution of carbonate defects in hydroxyapatite. Biomaterials, 27, 2150–2161.
Rey, C., Collins, B., Goehl, T., Dickson, I.R., and Glimcher, M.J. (1989) The carbonate environment in bone mineral: A resolution-enhanced Fourier transform infrared study. Calcified Tissue International, 45, 157–164.
Rey, C., Renugopalakrishnan, V., Shimizu, M., Collins, B., and Glimcher, M.J. (1991) A resolution-enhanced Fourier transform infrared spectroscopic study of the environment of the CO_3^{2-} ion in the mineral phase of enamel during its formation and maturation. Calcified Tissue International, 49, 259–268.
Siemens (1993) SHELXTL PC (Version 4.1). Siemens Analytical X-ray Instruments, Inc., Madison, Wisconsin, U.S.A.
Smyth, J.R. and Bish, D.L. (1988) Crystal Structures and Cation Sites of the Rock-Forming Minerals, 332 p. Allen and Unwin, London.
Suetsugu, Y., Shimoya, I., and Tanaka, J. (1998) Configuration of carbonate ions in apatite structure determined by polarized infrared spectroscopy. Journal of the American Ceramic Society, 81, 746–748.
Suetsugu, Y., Takahashi, Y., Okamura, F.P., and Tanaka, J. (2000) Structure analysis of A-type carbonate apatite by a single-crystal X-ray diffraction method. Journal of Solid State Chemistry, 155, 292–297.
Tonegawa, T., Ikoma, T., Yoshioka, T., Hanagata, N., and Tanaka, J. (2010) Crystal structure refinement of A-type carbonate apatite by X-ray powder diffraction. Journal of Materials Science, 45, 2419–2426.
Vignoles, M., Bonel, G., Holcomb, D.W., and Young, R.A. (1988) Influence of preparation conditions on the composition of type B carbonated hdroxyapatite and on the localization of the carbonate ions. Calcified Tissue International, 43, 33–40.
White, T.J., Ferraris, C., Kim, J., and Madhavi, S. (2005) Apatite: An adaptive framework structure. In G. Ferraris and S. Merlino, Eds., Micro- and Mesoporous Mineral Phases, 57, p. 307–373. Reviews in Mineralogy and Geochemistry, Mineralogical Society of America and the Geochemical Society, Chantilly, Virginia.
Wilson, R.M., Elliott, J.C., and Dowker, S.E.P. (1999) Rietveld refinement of the crystallographic structure of human dental enamel apatites. American Mineralogist, 84, 1406–1414.
Wilson, R.M., Elliott, J.C., Dowker, S.E.P., and Smith, R.I. (2004) Rietveld structure refinement of precipitated carbonate apatite using neutron diffraction data. Biomaterials, 25, 2205–2213.
Wilson, R.M., Dowker, S.E.P., and Elliott, J.C. (2006) Rietveld refinements and spectroscopic structural studies of a Na-free carbonate apatite made by hydrolysis of monetite. Biomaterials, 27, 4682–4692.
Wopenka, B. and Pasteris, J.D. (2005) A mineralogical perspective on the apatite in bone. Materials Science and Engineering, C, 25, 131–143.

Manuscript received September 3, 2010
Manuscript accepted February 8, 2011
Manuscript handled by Aaron Celestian